BIW10 Preprint -- Edited; preliminary green dot status
Final version will appear on JACoW

CHERENKOV RING TO OBSERVE LONGITUDINAL PHASE SPACE OF A LOW ENERGY ELECTRON BEAM EXTRACTED FROM RF GUN *

H. Hama#, K. Nanbu, M. Kawai, S. Kashiwagi, F. Hinode, T. Muto, F. Miyahara, Y. Tanaka
Research Centre for Electron Photon Science, Tohoku University
1-2-1 Mikamine, Taihaku-ku, Sendai 982-0826, Japan

Abstract

Particle distribution of the electron beam extracted from a thermionic RF gun in longitudinal phase space is crucial for electron bunch compression. Because space charge effects in the RF gun are not fully understood, an efficient bunch compression scheme employing magnetic chicane or alpha (α-) magnet is not easily designed. In order to measure the distribution in the longitudinal phase space of relatively lower energy electrons (below 2 MeV), we have studied a novel method for direct observation of electron energy employing velocity dependence of opening angle of Cherenkov radiation. Intrinsic energy and temporal resolution are discussed by showing a numerical ray-trace simulation.

ITC-RF GUN FOR FEMTO-SECOND ELECTRON PULSE

An intense terahertz radiation source based on an electron accelerator has been developed at Tohoku University, and is called the t-ACTS project [1]. Coherent THz radiation from an isochronous ring will be provided to multiple users simultaneously as a wide-band short-pulse source. Furthermore, a free electron laser (FEL) in the THz region driven by shorter electron pulses (less than the resonant wavelength) has been studied [2], in which a theoretical simulation suggests that FEL interaction can continuously amplifies the head part of radiation pulse when the cavity length is completely tuned. Stable production of very short electron bunches is a key issue for the t-ACTS project. Photoinjectors have already successfully produced femtosecond pulses with considerable bunch charge. However, we have chosen thermionic cathode for the RF gun because of stability, multi-bunch operation, and cheaper cost. Although the bunch charge will be small (a couple of tens of pC), and then coherent enhancement of the radiation is not so strong, the space charge effect may not be a very serious concern, and the thermionic cathode should have good stability, so excellent beam quality would be expected. Moreover, high repetition operation in multi-bunch mode will open another aspect of application experiments.

The thermionic RF gun consists of two independent cavity cells to manipulate the longitudinal beam phase space (see Fig. 1), so it is named the ITC (Independently-Tunable Cells) RF gun [3]. Particle distribution in longitudinal phase space is very important for the bunch compression including the space charge effect. The ITC-RF gun has been designed so as to produce appropriate longitudinal particle distribution by changing the relative RF phase and field strengths as shown in Fig. 2.

In order to optimize the parameters for the gun, such as field strengths and phase difference between two cells, we have done some numerical simulations of the beam production for the ITC-RF gun. Because a considerable part of the charge is concentrated into the head of the extracted beam, the space charge effect acts to deviate the electron distribution from a simple smooth line. This phenomenon is difficult to understand because different

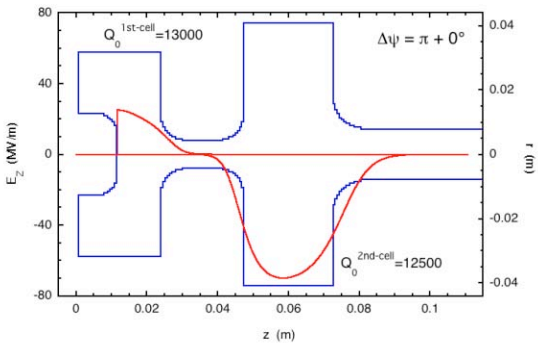

Figure 1: ITC-RF gun. A small size (ϕ = 1.85 mm) cathode of single crystal LaB_6 is employed, which can provide a beam current density of more than 50 A/cm^2.

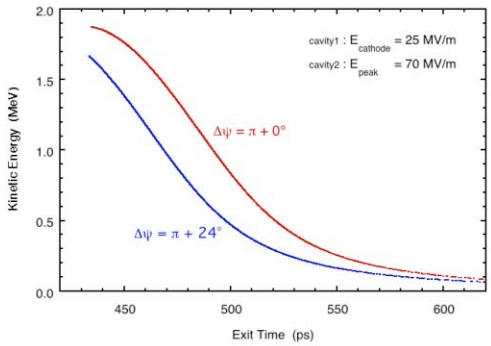

Figure 2: Particle distribution in the longitudinal phase space calculated by an FDTD code [4]. One for the phase difference of π + 0° (usual RF gun) leads higher energy. Meanwhile linear particle distribution results from phase space manipulation performed by phase tuning. Cathode current is 1.34 A for both calculations.

*Work supported by Grant-in-Aid for Scientific Research (S), the Ministry of Education, Science, Technology, Sports and Culture, Japan, Ccontact No. 20226003.
#hama@lns.tohoku.ac.jp

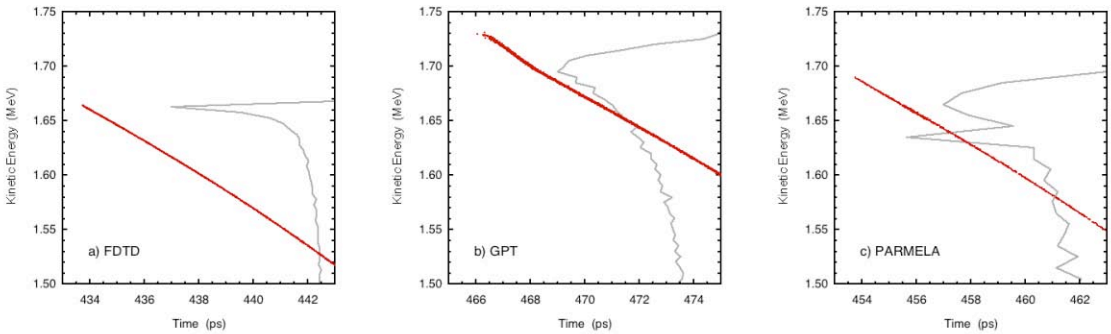

Figure 3: Longitudinal phase spaces calculated by a) the FDTD code, b) GPT, and c) PARMELA [5]. Parameters of the cavities are identical to those in Fig. 2 (the phase difference is π + 24°). Because of small differences in input geometry, the absolute energies are not the same, nor are the time origins. Although the slopes of the particle distributions are apparently in almost the same trend, the distributions around the top energy are very much different. Each code employs its own method for evaluation of the space charge effect, of course.

codes give different results as shown in Fig. 3, though almost the same results have been obtained when the particle charge is set to be zero. The phase space distribution calculated by PARMELA looks like that from the FDTD code. However, one can see a significant difference in the energy spectra, and some structure can be seen in that of PAMELA. The energy spectrum of GPT is much broader than that of FDTD, and there is a small bend in the phase space distribution.

In this study we are not going to pursue details of the simulation codes and correctness of the space charge models. We have, however, considered that direct measurement of the particle distribution in the longitudinal phase space is crucial for designing of the bunch compression scheme as well as understanding of the space charge effect.

CHERENKOV RING RADIATED FROM MeV ELECTRONS

As shown in Figs. 2 and 3, the beam energy from the ITC-RF gun is not so high (kinetic energy $T \sim 1.7$ MeV) and velocity is still slower than light, which means the particle distribution in the phase space may vary even in drift spaces due to the space charge force. Consequently a conventional analyzer magnet is not suitable for measurement of the particle energy because a considerable path length is inevitably required.

Cherenkov light is widely used for beam diagnostics and particle counters. It is well known that the Cherenkov angle θ_c is inversely proportional to the particle velocity β as

$$\cos\theta_c = 1/n(\omega)\beta, \qquad (1)$$

where $n(\omega)$ is the refractive index of the Cherenkov radiator medium at a radiation frequency ω [6]. The Frank-Tamm formula gives the energy dissipation of Cherenkov radiation with a frequency region from ω_1 to ω_2 as,

$$\frac{dE}{dz} = \frac{q^2}{4\pi}\int_{\omega_1}^{\omega_2} \mu(\omega)\omega\left(1-\cos^2\theta_c\right)d\omega, \qquad (2)$$

where z is the radiator length, q is the charge of the particle and $\mu(\omega)$ is the permeability of the medium. Assuming no frequency dependences of n and μ in a narrow band, the number of photons between wavelengths λ_1 and λ_2 emitted from an electron is expressed as

$$N = 2\pi\alpha z\left(\frac{1}{\lambda_1}-\frac{1}{\lambda_2}\right)\sin^2\theta_c, \qquad (3)$$

where α is the fine structure constant.

As one notices from Eqs. (1) and (3), the refractive index is an important parameter for detection of the particle energy. In order to secure sufficient energy resolution in the measurement system, a derivative of Cherenkov angle $d\theta_c/d\beta$ is preferred to be large. Meanwhile the intensity of the radiation is proportional to $\sin^2\theta_c$. Figure 4 shows the Cherenkov angle and the value of $\sin^2\theta_c$ calculated for a kinetic energy region from 1.4 to 2.0 MeV. The number of photons increases with n; meanwhile the slope of the Cherenkov angle is

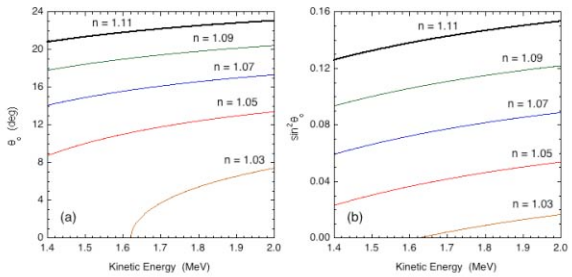

Figure 4: (a) The Cherenkov angle and (b) the value of $\sin^2\theta_c$ for various refraction indexes, plotted as a function of the kinetic energy.

gradually decreasing. Silica-aerogel has been presumed to be the radiator medium. We insist on the energy resolution and the angular resolution, so a refraction index of 1.05 has been chosen for further study. Sufficiently transparent aerogel having a higher refraction index is difficult to make.

OPTICAL ELEMENTS IN MEASUREMENT SYSTEM, LFC-CAMERA

Design Concept

Since the Cherenkov angle contains information of the particle energy, the photons having the same Cherenkov angle has to be focused on a certain position of a detector. If the focus points of different energies are aligned on a straight line, the energy distribution of the beam can be observed at once by using a semiconductor sensor. Furthermore, if information on relative arrival times into the aerogel for each particle can be preserved, we shall perform direct observation of the longitudinal phase space distribution by using a high-resolution streak camera.

The estimated photon number emitted from a single electron passing through a radiator medium of n = 1.05 with a thickness of z_R = 1 mm is approximately 0.04 for 1% bandwidth at a wavelength around 500 nm. In other words, a 1 pC bunch produces more than 200k photons. This seems to be enough to detect a single micro-pulse of the beam, because the total bunch charge of the energy range above 98% of the top energy is 20 ~ 30 pC for typical operation of the ITC-RF gun shown in Fig. 3.

Figure 5 shows a tentative optical apparatus design of the detection system we call the Linear Focal Cherenkov ring camera (LFC-camera). A turtle-back mirror gathers a part of the Cherenkov ring and confines onto the s-axis.

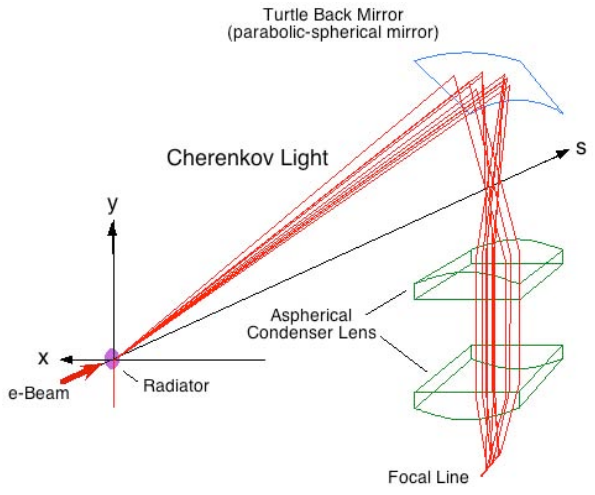

Figure 5: Schematic apparatus of the LFC-camera. The system consists of a specific (parabolic-spherical) mirror and two aspherical condenser lenses. Angular distribution of the Cherenkov radiation is imprinted onto a straight focal line.

The photons are transported and confined again by aspherical lenses. The Cherenkov angle is therefore converted into a position on a focal line.

Turtle-back Mirror

The reflecting surface of the mirror able to gather the photons of the Cherenkov ring and confine them onto a focal line is parabolic in the s-axis and spherical in the x-axis, which looks like a turtle-back carapace. As shown in Fig. 6, using a base position $(0, y_0, s_0)$ the mirror surface is expressed as

$$x^2 + y^2 - \left(-\frac{1}{2A} s^2 + \frac{A}{2} \right)^2 = 0 \quad \left(A \equiv \sqrt{{y_0}^2 + {s_0}^2} + y_0 \right). \tag{4}$$

Here, the base point has been chosen so as to make the system compact, i.e., the Cherenkov light from the electrons with a kinetic energy of 1.7 MeV hits the mirror at s_0= 0.3 m (then θ_c = 11.8 ° and y_0= 0.063 m).

Since the turtle-back mirror gives a focal line on the s-axis, indeed the beam axis, the photons have to be transported to outside of the beam pipe and confined again. We have intended to employ optical lenses for transport of the light and a normal incidence band-pass filter for wavelength selection because of convenience. However, spherical aberration of the lenses would be a severe issue when we like to gather the photons emitted across a large solid angle.

Aspherical Condenser Lens

Because a conventional formula of aspherical surface for the optical lenses contains many parameters, if one would like to eliminate aberration considerably, it may take a very long time to optimize the lens surface. For the moment we have designed a simple condenser lens consist of a flat surface and a one-dimensional aspherical surface, as shown in Fig. 5. The formula used to determine the surface is

$$x^2 + \left(y + g x^2 \right)^2 - \left(\frac{R}{\eta - 1} + g x^2 \right)^2 = 0, \tag{5}$$

where g is an aspherical coefficient, R is a base spherical

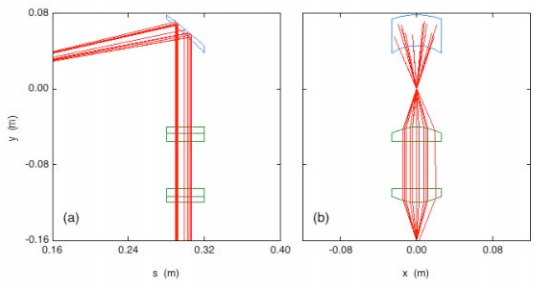

Figure 6: (a) Side view and (b) rear view of the light transport in the LFC-Camera. Red lines are light trajectories calculated by a ray-trace code assuming a point source.

curvature radius. The relative refractive index η of the lens is chosen to be 2.0, and R = 4 cm is employed in order to keep the system compact. Consequently it has turned out that the maximum acceptance can be obtained at $g \cong 23$, and approximately 10 % of the Cherenkov light emitted into the azimuthal angle of 2π is confined on the focal line 100 μm in width.

In Fig. 6, an example of calculation results from a ray-trace code we developed for ourselves is shown. As one can see in Fig. 6(b), the light passing through the far side of the lens goes out of the focal line.

CONSIDERATION FOR ENERGY AND TIME RESOLUTIONS OF LFC-CAMERA

Energy Dependence of the Focal Position

Using Eqs. (1) and (4), one can derive the focal position s_f at a particle velocity as

$$s_f(\beta) = An\beta\left(1-\sqrt{1-\left(\frac{1}{n\beta}\right)^2}\right). \qquad (6)$$

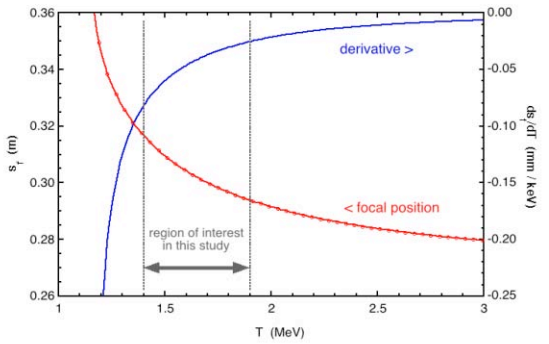

Figure 7: Red line indicates the focal position calculated using Eq. (6), and circles are results from the ray-trace code. Blue line denotes the derivative of the focal position with respect to the kinetic energy.

In Fig. 7, the focal position is plotted as a function of the kinetic energy, and its derivative ds_f/dT is also shown. Pixel size of recent CCD or CMOS is surprisingly smaller than 10 μm. That is sufficient for detection with an energy resolution of keV order, even in the 3-MeV region, if the radiation is coming from a point source.

Effect of Beam Emittance

Though transverse emittance of the beam from the RF gun is expected to be small, the finite spatial and angular spread of the beam may affect the energy resolution of the LFC-camera. We have assumed that the minimum normalized slice-emittance is equivalent to the thermal emittance of the cathode that is estimated to be about 2.5 x 10^{-7} m • rad for the ITC-RF gun. In order to evaluate the effect for the position resolution, the ray-trace calculations were performed for two different mono-

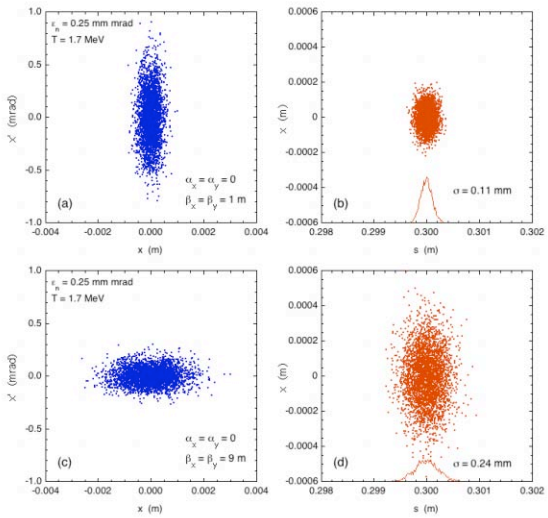

Figure 8: Particle distribution in the transverse phase space at the radiator (a) and photon distribution at the focal position (b) for a beta function of β = 1 m. Lower figures (c) and (d) are for β = 9 m.

energetic beam conditions characterized by a beta function of the Twiss parameter, such as tight focused beam on the radiator medium (β = 1 m) and loose focused one (β = 9 m).

Spreads of the focal position were 0.11 and 0.24 mm (standard deviation), respectively, as shown in Fig. 8. Since $|ds_f/dT|$ around T = 1.37 MeV is 0.037 mm/keV, those values correspond approximately to energy resolutions of 3 and 6 keV, respectively. We recognized that spatial electron distribution at the radiator mainly causes spread of the focal position, but it is less significant than we initially anticipated. We have also examined lower energies such as T = 1.4 MeV, and β = 1 m obtained energy resolutions of 2 and 4 keV, respectively. It can be concluded that the thermal emittance of the beam does not affect the energy resolution so much if we focus the beam on the radiator somewhat.

Effect of Thickness of the Radiator

Another important factor to be considered toward the energy resolution is a longitudinal position of the source point. We have supposed that the radiator thickness of z_R = 1 mm would be enough to produce sufficient number of Cherenkov photons. However, as discussed above, the spread of 1 mm on the focal line gives an energy width of ~ 30 keV at T = 1.7 keV, which is not negligibly small. If we need a thicker radiator than 1 mm, it is a matter of grave concern.

Performing the ray-trace calculation, it turned out that the turtle-back mirror gives a longitudinal focusing effect for different longitudinal source positions. Accordingly, the radiator thickness does not make considerable spread of the focal position.

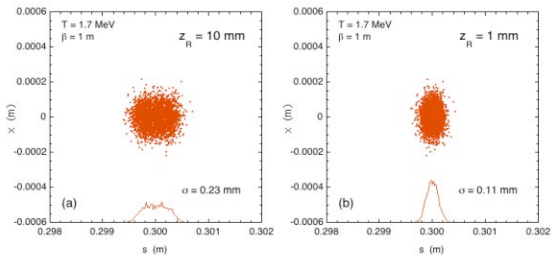

Figure 9: Focal position spread for the radiator thicknesses of (a) 10 and (b) 1 mm. The beam transverse distribution on the radiator is same as in Fig. 8(a). Refraction at the radiator surface is ignored because of the small refraction index.

As shown in Fig. 9, even the radiator of z_R = 10 mm causes a little position spread. For a case of z_R = 1 mm, we cannot see more than the beam emittance effect. This effect had not been anticipated initially but is quite acceptable because the parallel rays from the different sources are brought into a focus due to the parabolic mirror.

Time Resolution

The turtle-back mirror has been designed so as to eliminate path length difference of the rays from a single source to the 1st focal line (on the s-axis). However, deviation of the path length in the light transport and the speed of light in the aspherical condenser lenses, as well as the spatial beam distribution at the radiator, cause an intrinsic time resolution of the LFC-camera. Arrival time of the light onto the final focal line measured from the electron as it passes through the centre of the radiator medium has been derived from the ray-trace result. The arrival time was fund to have a small correlation with the longitudinal focal position, but not with the horizontal position. This fact suggests the light transport via the aspherical lenses does not affect the path length deviation so much. As shown in Fig. 10, even using a thicker radiator such as 10 mm, the intrinsic time resolution is a couple of hundred femtoseconds.

SUMMARY AND PROSPECT

We have designed a novel system for measurement of the longitudinal phase space distribution of the relatively lower energy electrons extracted from a thermionic RF

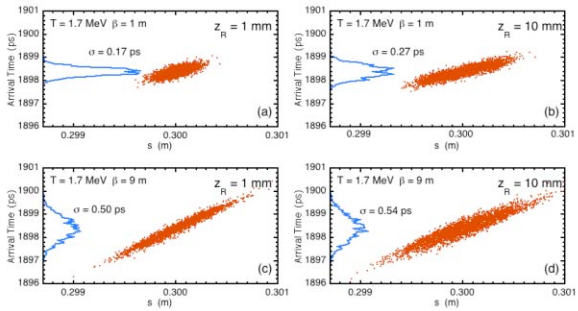

Figure 10: Two-dimensional plots of the arrival time and the longitudinal focal position. Upper figures are for β = 1 m, but for two different radiator thicknesses, (a) z_R = 1 mm and (b) z_R = 10 mm. Lower ones are for β = 9 m.

gun. The system, the LFC-camera, consists of a turtle-back mirror to confine the Cherenkov ring onto a focal line and two aspherical lenses for the light transportation. Using realistic electron distributions in phase space, the numerical ray-trace was performed. Though intrinsic energy resolution and time resolution of the optical system depend on both the beam transverse size and the thickness of the radiator, those have been easily suppressed to be less than 10 keV and 0.5 ps, respectively.

We are going to continue optimization of the optical element such as aspherical lenses and to study combined use with a streak camera.

REFERENCES

[1] H. Hama et al., N. J. of Phys. 8 (2006) 292; H. Hama et al., Nucl. Instr. and Meth. A, in press.
[2] M. Yasuda, Master thesis, "Simulation study of free electron laser employing very short electron bunches", Tohoku University (2009).
[3] T. Tanaka et al., Proc. 27th Int. FEL Conf., Stanford (2005) 371.
[4] H. Hama et al., Nucl. Instr. and Meth. A 528 (2004) 371.
[5] L. M. Young and J. H. Billen, "Parmela documentation", LA-UR-96-1835, revised July 17, 2003; GPT code, http://www.pulsar.nl/gpt/index.html.
[6] J. V. Julley, "Cherenkov Radiation and Its Application", Pergamon, New York (1958) 22.